

Research Paper

Uptake of ANG1005, A Novel Paclitaxel Derivative, Through the Blood-Brain Barrier into Brain and Experimental Brain Metastases of Breast Cancer

Fancy C. Thomas,¹ Kunal Taskar,¹ Vinay Rudraraju,¹ Satyanarayana Goda,¹ Helen R. Thorsheim,¹ Julie A. Gaasch,^{1,3} Rajendar K. Mittapalli,¹ Diane Palmieri,² Patricia S. Steeg,² Paul R. Lockman,¹ and Quentin R. Smith^{1,4}

Received May 28, 2009; accepted August 21, 2009; published online September 23, 2009

Purpose. We evaluated the uptake of angiopep-2 paclitaxel conjugate, ANG1005, into brain and brain metastases of breast cancer in rodents. Most anticancer drugs show poor delivery to brain tumors due to limited transport across the blood-brain barrier (BBB). To overcome this, a 19-amino acid peptide (angiopep-2) was developed that binds to low density lipoprotein receptor-related protein (LRP) receptors at the BBB and has the potential to deliver drugs to brain by receptor-mediated transport.

Methods. The transfer coefficient (K_{in}) for brain influx was measured by *in situ* rat brain perfusion. Drug distribution was determined at 30 min after i.v. injection in mice bearing intracerebral MDA-MB-231BR metastases of breast cancer.

Results. The BBB K_{in} for ¹²⁵I-ANG1005 uptake ($7.3 \pm 0.2 \times 10^{-3}$ mL/s/g) exceeded that for ³H-paclitaxel ($8.5 \pm 0.5 \times 10^{-5}$) by 86-fold. Over 70% of ¹²⁵I-ANG1005 tracer stayed in brain after capillary depletion or vascular washout. Brain ¹²⁵I-ANG1005 uptake was reduced by unlabeled angiopep-2 vector and by LRP ligands, consistent with receptor transport. *In vivo* uptake of ¹²⁵I-ANG1005 into vascularly corrected brain and brain metastases exceeded that of ¹⁴C-paclitaxel by 4–54-fold.

Conclusions. The results demonstrate that ANG1005 shows significantly improved delivery to brain and brain metastases of breast cancer compared to free paclitaxel.

KEY WORDS: ANG1005; blood-brain barrier; brain tumor; paclitaxel.

INTRODUCTION

The brain is not only a site of primary tumorigenesis (e.g., glioma) but is increasingly a site of cancer metastasis. Brain metastases are most common in lung and breast cancers, followed by melanoma (1). With advances in systemic chemotherapy, patients are responding to treatment and brain metastasis rates have soared—estimated at ~30% of Her-2+ and triple-negative cancers (2–4). The mainstays of brain metastasis treatment are whole-brain radiation, stereotactic radiation, and surgery, with corticosteroids and anticonvulsants for symptomatic management. However, none of these strategies work optimally. Prophylactic cranial radiation has been tested in randomized trials of lung cancer and reduced the probability of brain as a site of failure (5,6), but may be associated with a neurocognitive decline. A role for chemotherapy in brain

metastases has been difficult to establish. Multiple agents have been tested alone, in combination, or in combination with radiation, including temozolomide, lapatinib, capecitabine, vinorelbine, and taxanes (7–11). Few clinical responses and some disease stabilization have been reported. These data underscore the need for fresh approaches to drug penetration at the blood-brain (BBB) and blood-tumor (BTB) barriers.

The BBB is formed by a continuous monolayer of cerebrovascular endothelial cells joined together by tight junctions (12). For solutes to cross the BBB, they must either dissolve in and diffuse across the lipid endothelial cell membrane or be carried across by a carrier- or receptor-mediated transport (13). Unfortunately, most anticancer drugs show very limited uptake into brain following systemic administration (14,15). For example, paclitaxel, an agent used in the treatment of ovarian, breast, non-small cell lung and other cancers, reaches concentrations in brain that are 2–3 orders of magnitude less than those in most other tissues (16,17). Paclitaxel is kept out of brain in part by active efflux transport, the inhibition of which can raise brain paclitaxel concentrations by 6–10-fold (18–20). Overall, the BBB is estimated to limit the brain exposure of >95% of drugs through a combination of low passive permeability, active efflux transport, and biotransformation via phase I and II metabolism (21,22).

One approach to overcoming the BBB and BTB is to design drugs that are shuttled into brain using receptors that are naturally expressed at the BBB. This approach has been

¹Department of Pharmaceutical Sciences, Texas Tech University Health Sciences Center, 1300 South Coulter Drive, Suite 400, Amarillo, TX 79106, USA.

²Women's Cancers Section, Laboratory of Molecular Pharmacology, National Cancer Institute, National Institutes of Health, Bethesda, MD 20892, USA.

³Department of Life, Earth and Environmental Sciences, West Texas A & M University, Canyon, TX 79016, USA.

⁴To whom correspondence should be addressed. (e-mail: Quentin.Smith@ttuhsc.edu)

shown in animals to be successful with antibodies to the transferrin and insulin receptors (23). Another receptor that recently has been targeted for tissue drug delivery (24) is the low density lipoprotein receptor-related protein (LRP-1), one of a family of low density lipoprotein receptors involved in endocytotic uptake (25). LRP-1 is highly expressed at the BBB, has a rapid rate of endocytosis ($t_{1/2} < 30$ s), and is upregulated in brain tumors (25,26). It has been linked with BBB transcytosis of several proteins and peptides, including β -amyloid, tissue plasminogen activator (tPA), melanotransferrin, and receptor-associated peptide (RAP) (24,27,28).

Demeule et al. developed a series of 19 amino acid peptides called “angiopeps” targeted to the LRP-1 receptor. One of these peptides, angiopep-2, shows enhanced transcytosis across a brain endothelial monolayer system *in vitro* and improved brain uptake by *in situ* perfusion (29,30). This raises the question of whether drugs could be attached to angiopep-2 for transcytosis across the BBB. ANG1005, a peptide-paclitaxel conjugate with 3 molecules of paclitaxel linked to angiopep-2, has been shown to have activity against subcutaneously implanted glioblastoma and lung tumors, and to extend the survival of mice with intracerebral tumors (31). However, no studies have been reported on the mechanism of ANG1005 transport at the BBB or the extent to which it is accumulated in brain metastases *in vivo*. In this study we 1) determined the uptake of ^{125}I -ANG1005 into brain metastases of breast cancer and 2) evaluated BBB transport, self-saturation, and inhibition to gain insight as to the mechanism of translocation across brain endothelial cells. We report the ability of ^{125}I -ANG1005, ^{125}I -angiopep-2, and ^3H -paclitaxel to be taken up into brain by *in situ* perfusion, and compare the brain distribution of ^{125}I -ANG1005 to that of free ^{14}C -paclitaxel following intravenous injection in animals with brain metastases of breast cancer using quantitative autoradiography.

MATERIALS AND METHODS

Chemicals

^3H -Paclitaxel (10.7 Ci/mmol), ^{14}C -paclitaxel (53.3 mCi/mmol), ^{14}C -dextran (70 kD, 1.1 mCi/g) and ^{14}C -sucrose (498 mCi/mmol) were purchased from Moravex Biochemicals Inc (Brea, CA, USA). ANG1005 and angiopep-2 were a generous gift from Angiochem Inc. (Montreal, Quebec, Canada) and were labeled with ^{125}I using iodobeads (29,30). The resulting products, ^{125}I -ANG1005 (204 mCi/mmol) and ^{125}I -angiopep-2, were purified to >99% by HPLC prior to use. The purity of ^{14}C -dextran was established by dialysis at 4°C for 24 h (20 kD dialysis membrane cutoff). Poly-L-lysine, L-phenylalanine, aprotinin, chlorpromazine hydrochloride, indomethacin, human serum albumin, and verapamil hydrochloride were obtained from Sigma-Aldrich (St. Louis, MO, USA). RAP was purchased from Oxford Biomedicals (Rochester Hills, MI, USA).

In Situ Brain Perfusion

The *in situ* rat brain perfusion technique (32,33) was used to study the brain uptake of ^{125}I -ANG1005, ^{125}I -angiopep-2 and ^3H -paclitaxel at the BBB. Male Sprague Dawley rats (200–250 g) (Charles River Laboratories, Wilmington, MA)

were anesthetized with 40 mg/kg, i.p. sodium pentobarbital (Nembutal, Abbott Laboratories, North Chicago, IL, USA). The neck region was shaved and the left common carotid artery was exposed. The left external carotid artery was ligated and a PE-60 catheter filled with heparinized 0.9% NaCl saline (100 IU/mL) was inserted into the left common carotid artery. A heating pad linked to a YSI feedback controller device (Yellow Springs Instruments, Yellow Springs, OH, USA) maintained rectal temperature at 37°C . The PE-60 catheter was attached to a four-way valve linked to two infusion syringes—one containing drug radiotracer and one tracer-free. Perfusion fluid consisted of bicarbonate-buffered physiological saline (32) in which were dissolved unlabeled compound and/or inhibitors. The perfusion syringes were mounted on a temperature-controlled (37°C), dual infusion pump (Harvard Biosciences, South Natick, MA, USA). In most experiments, brain vascular volume was determined simultaneously using ^{14}C -sucrose. Perfusion was started upon severing the heart to stop blood flow to the brain. Tracer-containing fluid was infused into the common carotid artery at 5 mL/min for a period of 15–300 s. At the end of tracer perfusion, the animal was either decapitated or the brain vasculature was washed out by switching to perfusion with tracer-free fluid for 15–900 s. At the end of this procedure, the brain was removed from the skull and dissected into regions, which were subsequently weighed (34). Brain samples as well as dual aliquots of perfusion fluid (50–100 μL) were counted for ^{125}I activity using a gamma counter (Cobra 600). Samples containing beta tracers were digested with 1 mL tissue solubilizer (Solvable, Perkin Elmer, Boston, MA, USA) at 55°C for 8 h prior to addition of 10 mL of scintillation cocktail (Scintisafe TM 30%, New Jersey, USA). ^3H and/or ^{14}C radioactivity were determined using dual-label liquid scintillation counting (Beckman LS 6500, Fullerton, CA, USA).

Capillary Depletion

To evaluate the extent to which ^{125}I -angiopep-2 and ^{125}I -ANG1005 cross the BBB, capillary depletion was performed as described by Triguero et al. (35). The brain was perfused with tracer saline for 120 s followed by a 30 s post-wash with tracer-free fluid. At the end of post-wash perfusion, the brain was rapidly harvested from the skull and the perfused hemisphere weighed. The hemisphere was homogenized in ice-cold perfusion buffer, following which 40% ice cold dextran was added. The mixture was rehomogenized and then centrifuged at $5400\times g$ for 15 min at 4°C . The supernatant and pellet were separated and counted for radioactivity with the supernatant representing brain parenchymal tracer and the pellet representing tracer sequestered by the BBB. Care was taken to complete all steps quickly and to maintain samples ice cold.

Ultrafiltration

The free fraction of ^{125}I -ANG1005 in perfusion fluid was determined by ultrafiltration. ^{125}I -ANG1005 was dissolved in 0.5 mL perfusion fluid containing 2.7% human serum albumin in a Centricon micropartition device with a MW cutoff of 10 kD (Amicon Bioseparations, Bedford, MA, USA). The solution was centrifuged at 37°C to filter 10% of total volume. Aliquots of initial solution, retentate, and

filtrate were analyzed for radiotracer by gamma counting. Matching samples were run using protein-free fluid. The free fraction was calculated as the tracer concentration in the filtrate divided by that in the initial solution after correction for filtration efficiency across the membrane.

Octanol Water Distribution Coefficient

Tracers were dissolved in 1 mL phosphate-buffered saline (20 mM, pH 7.4) and 1 mL of water-saturated octanol was added. The mixture was vortexed for 1 min, centrifuged for 2 min, and then allowed to separate into organic and aqueous phases. Duplicate 50 μ l aliquots were taken from each phase and counted for radioactivity. The log octanol-water distribution coefficient (LogD) was calculated as $\text{Log}[(\text{tracer concentration in octanol})/(\text{tracer concentration in saline})]$.

High Performance Liquid Chromatography (HPLC)

A Varian Prostar HPLC system (Model SD-200) with UV detection (Dynamax) was utilized to purify the ANG1005 and angiopep-2 radiotracers and later to study the stability of the tracers in brain and perfusion fluid. A reverse phase C-18 YMC-Pak ODS-AM, 5 μ m, 150 \times 4.6 mm column was utilized for analysis. The mobile phase consisted of a gradient system with water (mobile phase A) and acetonitrile (mobile phase B), both with 0.05 % trifluoroacetic acid (TFA). The system was started at a flow rate of 1 mL/min with 10% B and held for 4 min. The system was ramped to 65% B from 4 min to 9 min and held at 65% until 15 min and then brought back to 10% B. Eluent samples were collected every minute into glass test tubes and counted for radioactivity. Only specimens with >99% purity were utilized for *in vivo* or perfusion studies.

Brain Extraction of ANG1005

In situ brain perfusion with ^{125}I -ANG1005 was performed for 120 s at 5 mL/min. At the end of perfusion, the brain was rapidly removed from the skull and frozen in liquid nitrogen. The perfused (left) cerebral hemisphere was separated, weighed, and ground into a fine paste using a mortar and pestle in the presence of liquid nitrogen. Two mL of ice cold (4°C) perfusion fluid were added to facilitate removal of the sample into a plastic test tube on ice (BD Falcon, 15 mL high clarity polypropylene conical tube; 17 \times 120 mm). Then, 4 mL of ice-cold (4°C), acidified acetonitrile (pH 4) were added to precipitate proteins. The mixture was vortexed at 4°C for 5 min. All samples and solutions were maintained ice-cold throughout the procedure using an ice bucket. After mixing was completed, the test tube was centrifuged for 10 min at 3,000 g and 4°C. The supernatant obtained was pipetted into a clean 15 mL plastic test tube (BD Falcon), and a 20 μ l aliquot was collected for determination of tracer activity. The remaining reconstituted sample (~ 4 mL) was dried down using a nitrogen evaporator. The dehydrated sample was then reconstituted in 50 μ l acidified DMSO (pH 4) and 200 μ l of mobile phase (65:35 acetonitrile:water with 0.05% TFA). The reconstituted sample was injected onto the HPLC using a 250 μ l loop manual injector, and the method described above was used to separate and analyze the constituents.

In Vivo Tumor Animals

Female NuNu mice (Charles River Laboratories, Wilmington, MA) were anesthetized with isoflurane and inoculated with 175,000 MDA-MB-231 cells, previously selected for brain tropism (231-BR) and transfected with an EGFP construct (36,37) into the left cardiac ventricle in serum-free media. Tumors seeded the brain and were allowed to grow for 4–6 weeks. Animals then were anesthetized with sodium pentobarbital (50 mg/kg, i.p.) and administered ^{125}I -ANG1005 (10 mg/kg, 7.5 μ Ci/20 g animal) or ^{14}C -paclitaxel (12 mg/kg; 25 μ Ci/20 g animal) into the femoral vein as a bolus. Tracers were allowed to circulate for 20 min and then 3 kD Texas Red dextran (1.5 mg/mouse) was administered i.v. 10 min before death. Animals were euthanized by severing the cardiac ventricles and the brain was promptly removed from the skull and promptly frozen in isopentane (-70°C). Blood and plasma tracer concentrations at the time of death were determined by liquid scintillation or gamma counting. Frozen brain was cut into 20 μ m coronal sections onto glass slides and air-dried. Tissue sections were analyzed for green and red fluorescence using an Olympus MVX10 stereo microscope with appropriate chroma filters (Chroma Technology Corp., Rockingham VT) as follows: eGFP: bandpass filters - excitation = 470 \pm 40 nm, emission = 525 \pm 50, with a dichromatic mirror set at 495 nm; TX Red 3kDA dextran: bandpass filters - excitation = 560 \pm 55 nm, emission = 645 \pm 75 nm, and a dichromatic mirror at 595 nm, which inhibited the capture of emission wavelengths below 595 nm and allowed effective separation of the eGFP emission signal from the metastases. Tissue radioactivity was quantified using a Fujifilm FLA7000 phosphorimager and the MCID Analysis program (InterFocus Imaging, Cambridge, England) with ^{14}C or ^{125}I autoradiography standards (Amersham Biosciences). Tracer autoradiographs for both ^{125}I -ANG1005 and ^{14}C -paclitaxel were normalized to 7.5 μ Ci/20 g mouse. Tissues were corrected for residual blood tracer using vascular volumes determined by quantitative autoradiography in matching MDA-MB-231BR brain metastases and normal brain tissue in separate animals with ^{14}C -70kD dextran (5 μ Ci/animal i.v., 2 min circulation period) (38). All animal experiments were performed in compliance with an approved IACUC protocol, in accordance with the NIH Guide for the Care and Use of Laboratory Animals.

Statistics

Prism 5 software was used to analyze the data. Results were presented as mean \pm SEM or S.D.. Statistical significance was determined using one-way analysis of variance (ANOVA). All p-values are two-sided, and Dunnett's or Tukey's post hoc testing was used for multiple comparisons.

Calculations

The unidirectional transfer coefficients for drug uptake into brain (K_{in}) were calculated from the time course of drug accumulation during brain perfusion as (33)

$$\text{Brain Uptake Space} = Q_{br}/C_{pf} = K_{in} \times T + V_i \quad (1)$$

where Q_{br} is the quantity of radiotracer drug taken up into brain during perfusion, C_{pf} is the radiotracer drug concen-

tration in perfusion fluid, T = perfusion time, and V_v = brain vascular volume. In most perfusion experiments, the total measured quantity of radiotracer drug in brain (Q_{tot}) at the end of perfusion was corrected for that fraction of tracer in perfusion fluid within the brain vasculature using the following equation:

$$Q_{br} = Q_{tot} - V_v C_{pf} \quad (2)$$

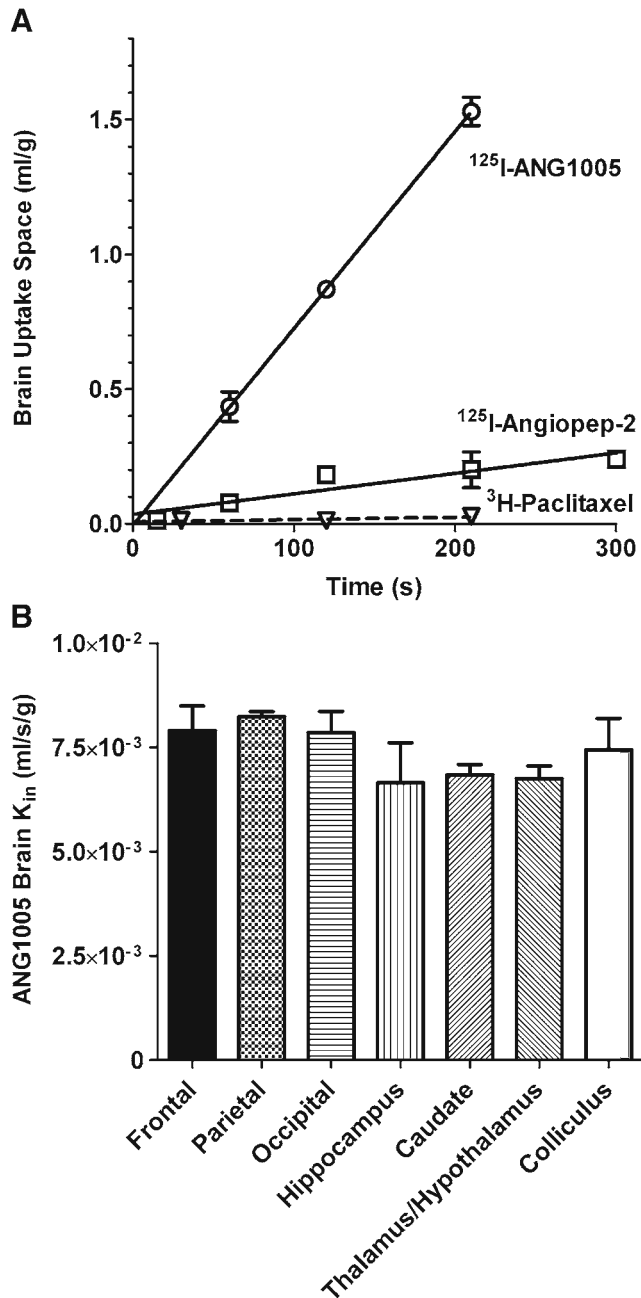


Fig. 1. Time course (A) of brain uptake of $^{125}\text{I-ANG1005}$, $^{125}\text{I-angiopep-2}$, and $^3\text{H-paclitaxel}$ during *in situ* brain perfusion. Data represent mean \pm SD ($n=3-6$ per group). Lines represent best fits to the data by least squares regression. Regional brain uptake (B) of $^{125}\text{I-ANG1005}$ during *in situ* brain perfusion with tracer saline. Data represent mean \pm SEM ($n=5$). Statistical significance was determined using ANOVA ($P>0.05$) for all seven well-perfused regions

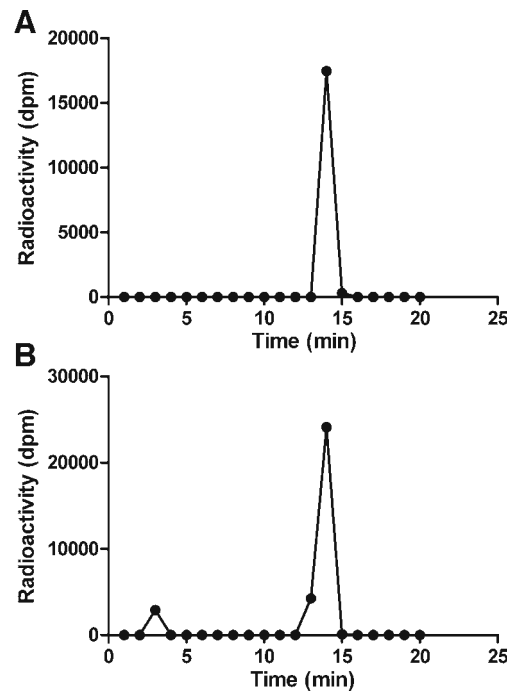


Fig. 2. HPLC chromatogram of $^{125}\text{I-ANG1005}$ in perfusion fluid (A) and brain (B) after perfusion uptake for 120 s. Intact $^{125}\text{I-ANG1005}$ eluted at 13–15 min. Tracer integrity in brain of tracer was $>95\%$

where V_v is the brain distribution space of $^{14}\text{C-sucrose}$ (32,33). In single time point experiments, K_{in} was derived as

$$K_{in} = [Q_{tot} - V_v C_{pf}] / C_{pf} T \quad (3)$$

In *in vivo* experiments, the total quantity of radiolabeled drug in brain and brain metastases was corrected for residual intravascular tracer by subtracting the product of the 2 min 70 kD $^{14}\text{C-dextran}$ distribution space (V_{bl}) and the blood drug tracer concentration at the time of death (C_{bl}) as

$$Q_{br} = Q_{tot} - V_{bl} C_{bl} \quad (4)$$

RESULTS

Time Course of Brain Uptake of ANG1005, Angiopep-2 and Paclitaxel and Regional Distribution of ANG1005

$^{125}\text{I-ANG1005}$, $^{125}\text{I-angiopep-2}$, and $^3\text{H-paclitaxel}$ showed linear, unidirectional uptake into brain from 15 to 300 s with BBB transfer coefficients (K_{in}) of $7.3 \pm 0.2 \times 10^{-3}$, $7.1 \pm 1.0 \times 10^{-4}$, and $8.5 \pm 0.5 \times 10^{-5}$ mL/s/g, respectively (Fig. 1A). Brain uptake at each time point was corrected for intravascular tracer using $^{14}\text{C-sucrose}$ ($V_v = 1.2 \pm 0.2 \times 10^{-2}$ mL/g). $^{125}\text{I-ANG1005}$ showed ~10- and 86-fold greater uptake K_{in} as compared to angiopep-2 and paclitaxel (Fig. 1A). Brain $^{14}\text{C-sucrose}$ space was not altered from control when determined in the presence of $^{125}\text{I-ANG1005}$ or $^{125}\text{I-angiopep-2}$ ($P>0.05$), indicating that angiopep peptide did not disrupt the permeability of the BBB. Based upon the time course of brain uptake, a perfusion time of 120 s was chosen for all subsequent experiments. The regional distribution of brain $^{125}\text{I-ANG1005}$ uptake was measured (Fig. 1B) and did not differ significantly ($P>0.05$) across all well-perfused regions of the cerebral hemisphere. After 2 min

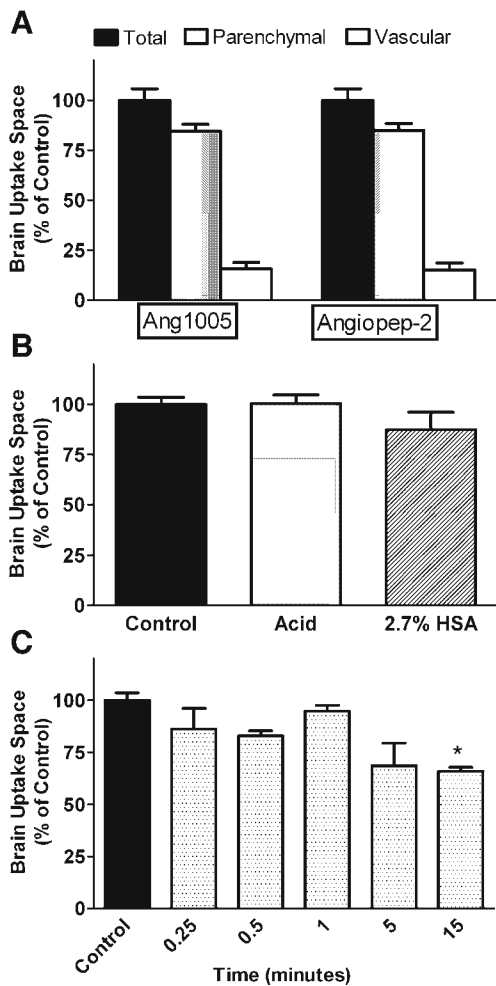


Fig. 3. Effect of capillary depletion (**A**), post-perfusion wash for 1 min with cold acidic saline (pH 3) or 2.7% human serum albumin fluid (**B**), or neutral saline wash for 1–15 min (**C**) on brain ^{125}I -angiopep-2 (**A**) or ^{125}I -ANG1005 (**A**, **B**, and **C**) after 120 s of uptake perfusion. Data represent mean \pm SEM ($n=3-5$ per group). * $P<0.05$

of perfusion, >90% of brain ^{125}I eluted by HPLC analysis as ^{125}I -ANG1005 (Fig. 2B), demonstrating that the tracer remained intact during perfusion and that uptake was not an artifact of tracer break-down into amino acid units (e.g., ^{125}I -iodotyrosine).

Effect of Capillary Depletion and Vascular Washout

Capillary depletion separates brain into brain parenchymal and vascular fractions (35) and is a simple method to estimate the extent to which a drug has crossed the BBB. As shown in Fig. 3A, >70% of brain ^{125}I -ANG1005 and ^{125}I -angiopep-2 distributed in the parenchymal fraction, whereas <30% associated with the vascular pellet. Similarly, 1 min post-perfusion wash with tracer-free neutral saline (pH 7.4), ice-cold acid saline (pH 3), or 2.7% albumin fluid was associated with a <15% ^{125}I -ANG1005 loss from brain (Fig. 3B and C). Cold acid wash has been used to differentiate between ligand binding and transport (39,40). Similarly, extending the period of neutral saline washout from 1 to 15 min only removed <30% of brain ^{125}I -ANG1005 tracer

(Fig. 3C), suggesting that the majority of tracer had been taken up into brain or brain endothelial cells, and was not simply binding to the luminal capillary endothelial surface.

Effect of Unlabeled Angiopep, LRP Ligand Competition, Cold Temperature, Serum Albumin, and Transport Inhibitors on Brain ^{125}I -ANG1005 Uptake

To determine if brain ^{125}I -ANG1005 uptake showed competition effects with angiopep-2 peptide, animals were perfused for 120 s with ^{125}I -ANG1005 saline containing 10 or 100 μM unlabeled angiopep-2 (Fig. 4A). Co-perfusion with unlabeled angiopep-2 reduced uptake by 30–40% ($P<0.05$). Similarly, co-perfusion with 10 μM aprotinin or 200 nM receptor-associated protein (RAP), ligands for LRP, reduced

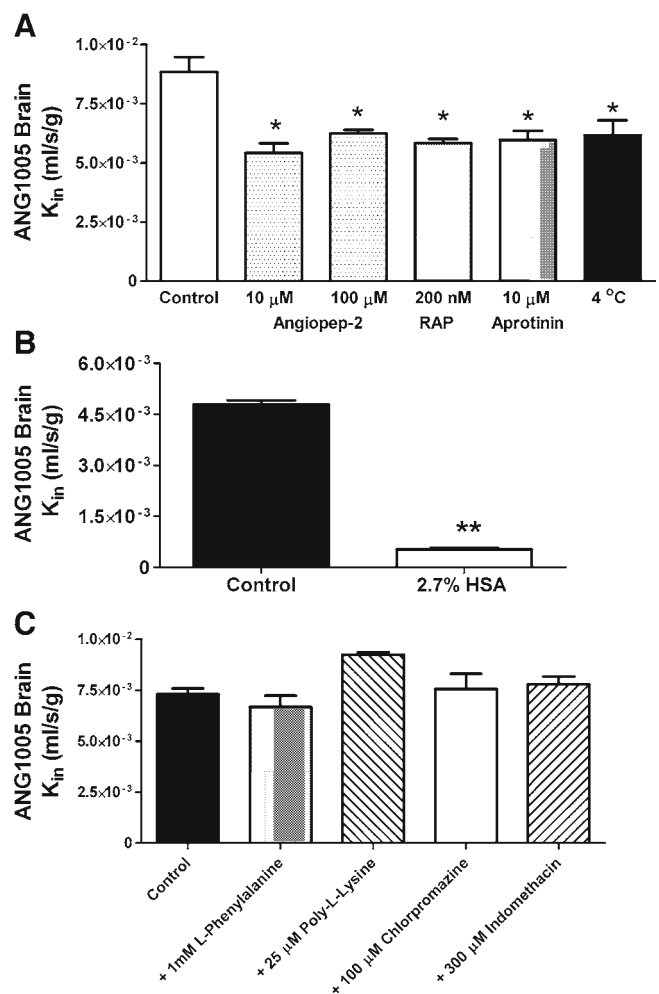


Fig. 4. (**A**)—Effect of co-perfusion with unlabeled angiopep-2, LRP ligands—aprotinin (10 μM) or RAP (200 nM), or cold temperature (4°C) on the brain uptake of ^{125}I -ANG1005. (**B**)—Effect of plasma protein (2.7% albumin) on brain uptake of ^{125}I -ANG1005. (**C**)—Effect of transport inhibitors or competitors, including L-phenylalanine (large neutral amino acid transport), poly-L-lysine (cationic absorption), and chlorpromazine and indomethacin (caveolae- and clathrin-mediated endocytosis), on BBB transport of ^{125}I -ANG1005. Data represent mean \pm SEM ($n=3-5$ per group). Statistical significance was determined using ANOVA with Dunnett's post hoc test in A and Student's t-test in B. * $P<0.05$. ** $P<0.01$

brain ^{125}I -ANG1005 uptake by a similar magnitude (Fig. 4A) ($P < 0.05$).

Receptor transcytosis has been reported to slow at reduced temperature. To test this, we pre-perfused the brain for 90 s with tracer-free ice-cold perfusion fluid to cool the brain. Then, the perfusate was switched to ice-cold perfusion fluid containing ^{125}I -ANG1005 for 120 seconds. Under these conditions, brain uptake of ^{125}I -ANG1005 decreased by 40%, similar to the effect seen with transport competitors (Fig. 4A). Together, the results supported the hypothesis of a component of saturable uptake transport at the BBB mediated by LRP.

^{125}I -ANG1005 was found to bind significantly to human serum albumin with a free fraction of $10 \pm 2\%$ in 2.7% albumin saline. Consistent with this, brain ^{125}I -ANG1005 uptake K_{in} decreased $\sim 90\%$ with 2.7% albumin saline perfusion fluid, as compared to protein-free saline (Fig. 4B) ($P < 0.05$).

To further investigate the mechanism by which ^{125}I -ANG1005 is taken up into brain, the effects of co-perfusion with transport inhibitors, including L-phenylalanine (1 mM), poly-L-lysine (25 μM), chlorpromazine (100 μM), and indomethacin (300 μM), were determined by *in situ* perfusion (Fig. 4C). None of the four agents produced a statistically significant decrease in the K_{in} for brain uptake of ^{125}I -ANG1005 ($P > 0.05$). L-phenylalanine blocks the large neutral amino acid transporter (LAT1) (41,42), poly-L-lysine reduces cationic absorptive-mediated transport (43), whereas indomethacin and chlorpromazine are inhibitors of caveolae- and clathrin-mediated endocytosis, respectively (44–46).

Brain Uptake in Mice Bearing Brain Metastases of Breast Cancer *In Vivo*

A brain-seeking derivative of the MDA-MB-231 (231-BR) human breast cancer cell line produces both large and small brain metastases upon intracardiac injection (36). Given the relevance of paclitaxel to breast cancer, we asked whether ANG1005 could more effectively penetrate brain metastases of breast cancer than the parent chemotherapeutic compound. Figure 5 shows the brain uptake of ^{125}I -ANG1005 and ^{14}C -paclitaxel in 231-BR tumor bearing mice. Tumor cells transfected with green fluorescent protein were visualized by fluorescence microscopy. Texas Red 3 kD dextran (red) was observed to leak from a proportion of metastases, indicating heterogeneity in BTB permeability in this model system. ^{125}I -ANG1005 uptake into brain exceeded that of free ^{14}C -paclitaxel by >10 -fold at equivalent radiotracer dose ($P < 0.05$). ^{125}I -ANG1005 concentration equaled 25.5 ± 0.8 nCi/g ($n=20$) in tumor-free brain at 30 min, whereas normalized ^{14}C -paclitaxel concentration (normalized to equivalent ^{125}I -ANG1005 radiotracer dose in $\mu\text{Ci}/\text{animal}$) equaled 1.2 ± 0.1 nCi/g ($n=11$) in tumor-free brain. The matching concentrations of ^{125}I -ANG1005 and ^{14}C -paclitaxel equaled 33.6 ± 2.7 nCi/g ($n=25$) and 4.6 ± 0.8 nCi/g ($n=21$) in brain metastases ($P < 0.05$).

Absolute brain and tumor radiotracer drug concentrations were converted, using matching tracer specific activities and molecular weights, to nmole drug/kg wet tissue weight at equivalent molar doses of the two agents (14 $\mu\text{mole}/\text{kg}$ mouse =

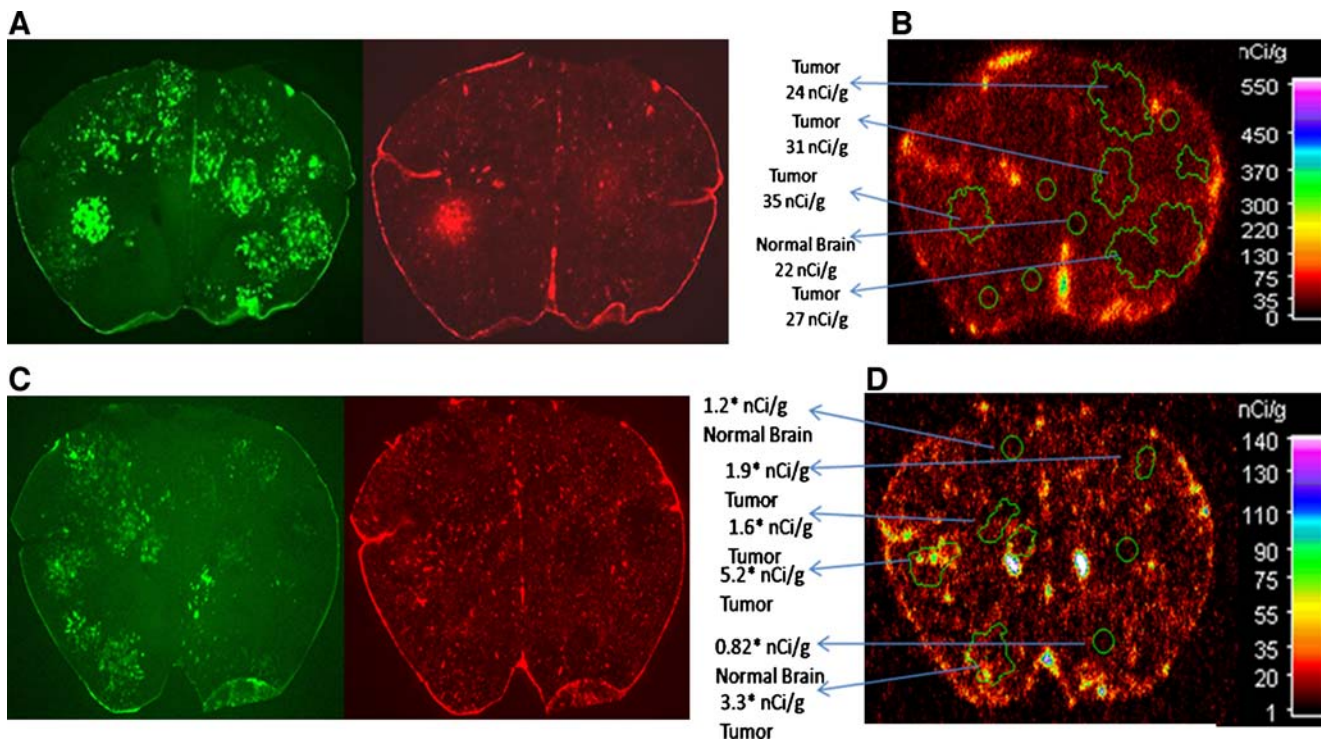


Fig. 5. Distribution of green fluorescent protein transfected 231-BR metastases of breast cancer (Green: **A** and **C**), Texas Red 3 kD dextran (Red: **A** and **C**), ^{125}I -ANG1005 (Quantitative autoradiograph, **B**), and ^{14}C -paclitaxel (Quantitative autoradiograph, **D**) in 20 μm coronal representative sections of brain. ^{125}I -ANG1005 and ^{14}C -paclitaxel were allowed to circulate *in vivo* after i.v. injection for 30 min. Texas Red dextran circulated for 10 min prior to death. Animals received equivalent drug doses; radioactivity was normalized to 7.5 $\mu\text{Ci}/\text{mouse}$

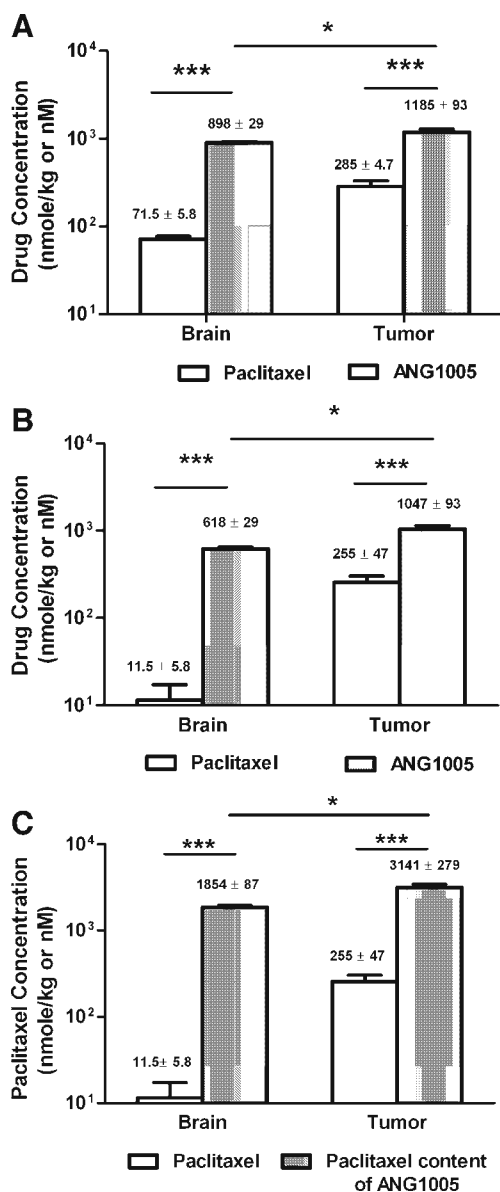


Fig. 6. Brain and brain metastasis molar (nmol/kg) concentrations of paclitaxel and ANG1005 at 30 min after injection *in vivo* in mice. Results were normalized to an equivalent drug dose of 14 μ mole/kg mouse (i.e., the dose for paclitaxel) and are expressed in nmole/kg wet tissue weight. **A**—Represents total tissue concentrations of paclitaxel or ANG1005; **B**—represents vascularly corrected tissue concentrations of paclitaxel or ANG1005; and **C**—represents vascularly corrected tissue concentrations expressed in terms of paclitaxel content (note—each mole of ANG1005 carries 3 moles of paclitaxel). Results are expressed as mean \pm SEM ($n=11-25$). * $P<0.05$ brain vs tumor for ANG1005. *** $P<0.05$ paclitaxel vs ANG1005 within the same tissue

dose of free paclitaxel in 25 mg/kg paclitaxel). Given that 1 kg tissue is approximately 1 L volume, this works out to approximate nM concentration. The results for this comparison are illustrated in Fig. 6. The absolute tissue concentrations in nmole/kg (Fig. 6A) showed comparable differences between the two drugs for tumor and brain as to that noted when concentrations were expressed in nCi/g (i.e., ANG1005 >10-fold paclitaxel in brain and ANG1005 >4-fold paclitaxel in brain metastases). Total tissue drug concentrations were corrected for residual

vascular drug by subtracting the product of vascular volume and terminal drug concentration in blood. Terminal blood concentration averaged 7,598 nmole/kg for paclitaxel and 35,442 nmole/kg for ANG1005. Mean vascular volumes by quantitative autoradiography were $0.79 \pm 0.10 \times 10^{-2}$ ml/g for normal brain ($n=35$) and $0.39 \pm 0.04 \times 10^{-2}$ ml/g for brain metastases ($n=35$). Vascular volume, on average, was significantly less in brain metastases than in normal brain in this model of brain metastatic cancer ($P<0.05$). Vascularly corrected drug concentrations are shown in Fig 6B for tumor and normal brain. Vascular correction lowered the brain drug content by ~84% for paclitaxel and 31% for ANG1005, whereas the impact was less for tumor. With this equimolar dose calculation, ANG1005 showed 54-fold greater brain distribution than similarly dosed paclitaxel, whereas the enhancement was 4-fold in brain metastasis. Adjusting for the fact that each ANG1005 holds 3 paclitaxel molecules, the absolute delivery of paclitaxel via ANG1005 was 161-fold greater for brain tissue and >12-fold greater for brain metastases (Fig. 6C). The results suggest significantly improved brain and brain metastasis delivery of paclitaxel with ANG1005 than with administration of free paclitaxel.

DISCUSSION

In the current study, we evaluated the brain uptake of 125 I-ANG1005, a novel peptide-paclitaxel conjugate designed to improve delivery of paclitaxel across the BBB. Using *in situ* rat brain perfusion, 125 I-ANG1005 showed significantly improved uptake into brain, with a $K_{in} >80$ -fold greater than paclitaxel and 1–3 orders of magnitude higher than other peptides and antibodies that show transport across the BBB (28,30,39,47,48).

In an attempt to determine whether the observed brain 125 I-ANG1005 uptake reflected binding to the vascular elements or transcytosis into brain, capillary depletion experiments as well as extensive post-perfusion washout experiments were conducted. One min post-perfusion with normal saline (pH 7.4), cold acid saline (pH 3), or 2.7% albumin produced only modest (<20%) reductions in brain 125 I-ANG1005 levels. Similarly, with capillary depletion, >70% of tracer was associated with the parenchymal fraction. This suggests that a significant fraction of ANG1005 may transcytose across the BBB and is not simply internalized or binding to the vascular endothelium. Such a finding is consistent with the proposed BBB transport mechanism for angiopep-2 as a drug delivery vector. However, 125 I-ANG1005 is clearly enriched in the microvascular fraction with 15–30% of tracer in the capillary pellet, even though the vascular elements make up <1% of brain. Thus, further studies of the ANG1005 transcytosis process over more extended time periods are merited, as the current study focused upon only the first 1–5 min.

Angiopep-2 was designed based on the binding domains of LRP and is presumed to be transcytosed into the brain by means of the LRP receptor (30). To examine whether the same mechanism is involved in the brain uptake of 125 I-ANG1005, we determined the brain uptake of 125 I-ANG1005 in the presence of unlabeled angiopep-2 and other LRP ligands. Perfusion with unlabeled angiopep-2 or LRP ligands, aprotinin and RAP, reduced brain 125 I-ANG1005 uptake, consistent with

a role of LRP receptor. However, the magnitude of these effects was only 30–40% suggesting that either 1) there may be more than one mechanism involved in brain uptake of ANG1005, or 2) the observed brain uptake signal may be a mixture of tight binding and transport, with transport comprising only 30–40% of the signal. A comparable reduction in brain ^{125}I -ANG1005 uptake was seen with perfusion with ice-cold perfusion buffer that slows transport and transcytosis processes. Demeule et al. (29,30) similarly found that initial brain uptake of ^{125}I -angiopep-2 could only be partially inhibited (40–50%) by excess unlabeled angiopep-2 peptide or LRP ligands. The nature of the remaining, uninhibited ANG1005 uptake component remains to be determined.

^{125}I -ANG1005 influx into brain was homogeneous across sampled brain regions, suggesting that angiopep-2 could be used to deliver drugs broadly to the whole cerebral hemisphere. Similarly, brain ^{125}I -ANG1005 uptake was not inhibited by L-phenylalanine or poly-L-lysine, demonstrating that the signal was not an artifact of contamination by iodotyrosine or mediated by simple absorptive-mediated endocytosis (41,43). The endocytosis inhibitors, chlorpromazine and indomethacin, failed to alter ANG1005 uptake into brain. However, the exposure period (2 min) may have been inadequate for the inhibitors to disrupt the endocytosis process. Most studies pre-incubate the inhibitors for 10–60 min prior to uptake measurement (44–46). In contrast, addition of 2.7% serum albumin to the perfusion fluid sharply reduced the free fraction of ^{125}I -ANG1005 in the perfusion buffer by 90% and similarly decreased ^{125}I -ANG1005 uptake into brain by *in situ* perfusion, suggesting that plasma protein binding significantly affects ANG1005 transport across the BBB. This matches what has been found for other drugs, including free paclitaxel, which bind restrictively to plasma proteins (49,50). The fact that the reduction in free fraction closely matched the reduction in total brain influx indicates that free (unbound) ANG1005 is the driving force for drug transport into brain (49). The magnitude of albumin-bound ANG1005 is considerable (90%), but less than that of free paclitaxel in serum (~98%) (51). However, the free fraction of ANG1005 may be less in serum due to the presence of other plasma proteins.

ANG1005, with three paclitaxel residues, showed ~161-fold greater uptake into brain than free drug paclitaxel at 30 min after i.v. injection *in vivo*. These results demonstrate that conjugating a drug, such as paclitaxel, that shows poor brain delivery with a carrier, such as angiopep-2, can significantly increase the drug's brain distribution. Further, our studies show a >10-fold increase in paclitaxel delivery to brain metastases through ANG1005 and that ANG1005 is shuttled into brain at least in part by an LRP-dependent mechanism. In the present studies, tumor-specific localization of ANG1005 was only slightly greater (1.5-fold or less) than surrounding normal brain, though the circulation time in our *in vivo* experiments was only 30 min. Many tumor cells show increased expression of LRP (29), and, thus the potential exists for long-term localization and retention based upon LRP-dependent transport and binding. Further, attachment of paclitaxel to angiopep overcomes active efflux mechanisms, such as p-glycoprotein (31). Thus, ANG1005 may benefit from reduced tissue and tumor exclusion from multidrug resistance transport mechanisms.

We conclude that ANG1005, a novel peptide-paclitaxel conjugate, can be successfully taken up into brain and may sidestep some of the poor brain bioavailability issues observed with classical anticancer drugs, such as paclitaxel. With increased brain availability, ANG1005 would be expected to show promise for the treatment of brain tumors. In fact, Regina et al. (31) have reported initial efficacy of ANG1005 in animal models against intracerebral glioblastoma and non-small-cell lung carcinoma.

Brain metastases of breast and other cancers represent an unmet medical need. Taxanes are widely used in the treatment of breast and other cancers. Systemic efficacy has been limited by formulation issues, the effects of multidrug resistance pumps and side effects. Efforts to improve taxane efficacy have included nanoparticle formulations (52) and local delivery using implantable controlled release biodegradable polymers (53). However, local implantable devices would require surgery and may not be effective in the metastatic situation, where multiple lesions often occur. ANG1005 may represent a preferred strategy, whereby multiple brain metastases could be treated without surgery. The present data suggest that this compound may have efficacy alone or in combination with radiation, which will be tested in future studies.

ACKNOWLEDGEMENTS

This work was supported by grants from the Department of Defense Breast Cancer Program (W81XWH-062-0033), NIH/NINDS (R01 NS052484), and from AngioChem, Inc.

REFERENCES

- Weil RJ, Palmieri DC, Bronder JL, Stark AM, Steeg PS. Breast cancer metastasis to the central nervous system. *Am J Pathol.* 2005;167:913–20.
- Clayton AJ, Danson S, Jolly S, Ryder WD, Burt PA, Stewart AL, et al. Incidence of cerebral metastases in patients treated with trastuzumab for metastatic breast cancer. *Br J Cancer.* 2004;91:639–43.
- Lin NU, Winer EP. Brain metastases: the HER2 paradigm. *Clin Cancer Res.* 2007;13:1648–55.
- Smid M, Wang Y, Zhang Y, Sieuwerts AM, Yu J, Klijn JG, et al. Subtypes of breast cancer show preferential site of relapse. *Cancer Res.* 2008;68:3108–14.
- Pottgen C, Eberhardt W, Grannass A, Korfee S, Stuben G, Teschler H, et al. Prophylactic cranial irradiation in operable stage IIIA non small-cell lung cancer treated with neoadjuvant chemoradiotherapy: results from a German multicenter randomized trial. *J Clin Oncol.* 2007;25:4987–92.
- Slotman B, Faivre-Finn C, Kramer G, Rankin E, Snee M, Hatton M, et al. Prophylactic cranial irradiation in extensive small-cell lung cancer. *N Engl J Med.* 2007;357:664–72.
- Addeo R, De Rosa C, Faiola V, Leo L, Cennamo G, Montella L, et al. Phase 2 trial of temozolomide using protracted low-dose and whole-brain radiotherapy for nonsmall cell lung cancer and breast cancer patients with brain metastases. *Cancer.* 2008;113:2524–31.
- Cassier PA, Ray-Coquard I, Sunyach MP, Lancry L, Guastalla JP, Ferlay C, et al. A phase 2 trial of whole-brain radiotherapy combined with intravenous chemotherapy in patients with brain metastases from breast cancer. *Cancer.* 2008;113:2532–8.
- Ekenel M, Hormigo AM, Peak S, Deangelis LM, Abrey LE. Capecitabine therapy of central nervous system metastases from breast cancer. *J Neurooncol.* 2007;85:223–7.

10. Lin NU, Carey LA, Liu MC, Younger J, Come SE, Ewend M, et al. Phase II trial of lapatinib for brain metastases in patients with human epidermal growth factor receptor 2-positive breast cancer. *J Clin Oncol*. 2008;26:1993–9.
11. Omuro AM, Raizer JJ, Demopoulos A, Malkin MG, Abrey LE. Vinorelbine combined with a protracted course of temozolomide for recurrent brain metastases: a phase I trial. *J Neurooncol*. 2006;78:277–80.
12. Deeken JF, Loscher W. The blood-brain barrier and cancer: transporters, treatment, and Trojan horses. *Clin Cancer Res*. 2007;13:1663–74.
13. Muldoon LL, Soussain C, Jahnke K, Johanson C, Siegal T, Smith QR, et al. Chemotherapy delivery issues in central nervous system malignancy: a reality check. *J Clin Oncol*. 2007;25:2295–305.
14. Motl S, Zhuang Y, Waters CM, Stewart CF. Pharmacokinetic considerations in the treatment of CNS tumours. *Clin Pharmacokinet*. 2006;45:871–903.
15. D.M. Peereboom. Chemotherapy in brain metastases. *Neurosurgery*. 57:S54–65; discussion S51–54 (2005).
16. Eiseman JL, Eddington ND, Leslie J, MacAuley C, Sentz DL, Zuhowski M, et al. Plasma pharmacokinetics and tissue distribution of paclitaxel in CD2F1 mice. *Cancer Chemother Pharmacol*. 1994;34:465–71.
17. Sparreboom A, van Tellingem O, Nooijen WJ, Beijnen JH. Tissue distribution, metabolism and excretion of paclitaxel in mice. *Anti Canc Drugs*. 1996;7:78–86.
18. Breedveld P, Beijnen JH, Schellens JH. Use of P-glycoprotein and BCRP inhibitors to improve oral bioavailability and CNS penetration of anticancer drugs. *Trends Pharmacol Sci*. 2006;27:17–24.
19. Fellner S, Bauer B, Miller DS, Schaffrik M, Fankhanel M, Spruss T, et al. Transport of paclitaxel (Taxol) across the blood-brain barrier in vitro and in vivo. *J Clin Invest*. 2002;110:1309–18.
20. Gallo JM, Li S, Guo P, Reed K, Ma J. The effect of P-glycoprotein on paclitaxel brain and brain tumor distribution in mice. *Cancer Res*. 2003;63:5114–7.
21. Dauchy S, Duthel F, Weaver RJ, Chassoux F, Daumas-Duport C, Couraud PO, et al. ABC transporters, cytochromes P450 and their main transcription factors: expression at the human blood-brain barrier. *J Neurochem*. 2008;107:1518–28.
22. Pardridge WM. The blood-brain barrier: bottleneck in brain drug development. *NeuroRx*. 2005;2:3–14.
23. Pardridge WM. Re-engineering biopharmaceuticals for delivery to brain with molecular Trojan horses. *Bioconjugate Chem*. 2008;19:1327–38.
24. de Boer AG, Gaillard PJ. Strategies to improve drug delivery across the blood-brain barrier. *Clin Pharmacokinet*. 2007;46:553–76.
25. Lillis AP, Van Duyn LB, Murphy-Ullrich JE, Strickland DK. LDL receptor-related protein 1: unique tissue-specific functions revealed by selective gene knockout studies. *Physiol Rev*. 2008;88:887–918.
26. Bu G, Maksymovitch EA, Geuze H, Schwartz AL. Subcellular localization and endocytic function of low density lipoprotein receptor-related protein in human glioblastoma cells. *J Biol Chem*. 1994;269:29874–82.
27. Demeule M, Poirier J, Jodoin J, Bertrand Y, Desrosiers RR, Dagenais C, et al. High transcytosis of melanotransferrin (P97) across the blood-brain barrier. *J Neurochem*. 2002;83:924–33.
28. Pan W, Kastin AJ, Zankel TC, van Kerkhof P, Terasaki T, Bu G. Efficient transfer of receptor-associated protein (RAP) across the blood-brain barrier. *J Cell Sci*. 2004;117:5071–8.
29. Demeule M, Currie JC, Bertrand Y, Che C, Nguyen T, Regina A, et al. Involvement of the low-density lipoprotein receptor-related protein in the transcytosis of the brain delivery vector angiopep-2. *J Neurochem*. 2008;106:1534–44.
30. Demeule M, Regina A, Che C, Poirier J, Nguyen T, Gabathuler R, et al. Identification and design of peptides as a new drug delivery system for the brain. *J Pharmacol Exp Ther*. 2008;324:1064–72.
31. Regina A, Demeule M, Che C, Lavallee I, Poirier J, Gabathuler R, et al. Antitumour activity of ANG1005, a conjugate between paclitaxel and the new brain delivery vector Angiopep-2. *Br J Pharmacol*. 2008;155:185–97.
32. Smith QR. Brain perfusion systems for studies of drug uptake and metabolism in the central nervous system. *Pharm Biotech*. 1996;8:285–307.
33. Smith QR. A review of blood-brain barrier transport techniques. *Meth Mol Med*. 2003;89:193–208.
34. Takasato Y, Rapoport SI, Smith QR. An in situ brain perfusion technique to study cerebrovascular transport in the rat. *Am J Physiol*. 1984;247:H484–93.
35. Triguero D, Buciak J, Pardridge WM. Capillary depletion method for quantification of blood-brain barrier transport of circulating peptides and plasma proteins. *J Neurochem*. 1990;54:1882–8.
36. Palmieri D, Bronder JL, Herring JM, Yoneda T, Weil RJ, Stark AM, et al. Her-2 overexpression increases the metastatic outgrowth of breast cancer cells in the brain. *Cancer Res*. 2007;67:4190–8.
37. Yoneda T, Williams PJ, Hiraga T, Niewolna M, Nishimura R. A bone-seeking clone exhibits different biological properties from the MDA-MB-231 parental human breast cancer cells and a brain-seeking clone in vivo and in vitro. *J Bone Miner Res*. 2001;16:1486–95.
38. Palmieri D, Ziylan YZ, Robinson PJ, Rapoport SI. Kinetics and distribution volumes for tracers of different sizes in the brain plasma space. *Brain Res*. 1988;462:1–9.
39. Zlokovic BV, Ghiso J, Mackic JB, McComb JG, Weiss MH, Frangione B. Blood-brain barrier transport of circulating Alzheimer's amyloid beta. *Biochem Biophys Res Comm*. 1993;197:1034–40.
40. Samii A, Bickel U, Stroth U, Pardridge WM. Blood-brain barrier transport of neuropeptides: analysis with a metabolically stable dermorphin analogue. *Am J Physiol*. 1994;267:E124–31.
41. Momma S, Aoyagi M, Rapoport SI, Smith QR. Phenylalanine transport across the blood-brain barrier as studied with the in situ brain perfusion technique. *J Neurochem*. 1987;48:1291–300.
42. Smith QR, Momma S, Aoyagi M, Rapoport SI. Kinetics of neutral amino acid transport across the blood-brain barrier. *J Neurochem*. 1987;49:1651–8.
43. Rousselle C, Smirnova M, Clair P, Lefauconnier JM, Chavanieu A, Calas B, et al. Enhanced delivery of doxorubicin into the brain via a peptide-vector-mediated strategy: saturation kinetics and specificity. *J Pharmacol Exp Ther*. 2001;296:124–31.
44. Yumoto R, Nishikawa H, Okamoto M, Katayama H, Nagai J, Takano M. Clathrin-mediated endocytosis of FITC-albumin in alveolar type II epithelial cell line RLE-6TN. *Am J Physiol*. 2006;290:L946–55.
45. Kim HR, Gil S, Andrieux K, Nicolas V, Appel M, Chacun H, et al. Low-density lipoprotein receptor-mediated endocytosis of PEGylated nanoparticles in rat brain endothelial cells. *Cell Mol Life Sci*. 2007;64:356–64.
46. Visser CC, Stevanovic S, Heleen Voorwinden L, Gaillard PJ, Crommelin DJ, Danhof M, et al. Validation of the transferrin receptor for drug targeting to brain capillary endothelial cells in vitro. *J Drug Target*. 2004;12:145–50.
47. Bickel U, Yoshikawa T, Pardridge WM. Delivery of peptides and proteins through the blood-brain barrier. *Adv Drug Del Rev*. 2001;46:247–79.
48. Pardridge WM, Kang YS, Buciak JL, Yang J. Human insulin receptor monoclonal antibody undergoes high affinity binding to human brain capillaries in vitro and rapid transcytosis through the blood-brain barrier in vivo in the primate. *Pharm Res*. 1995;12:807–16.
49. Mandula H, Parepally JM, Feng R, Smith QR. Role of site-specific binding to plasma albumin in drug availability to brain. *J Pharmacol Exp Ther*. 2006;317:667–75.
50. Parepally JM, Mandula H, Smith QR. Brain uptake of non-steroidal anti-inflammatory drugs: ibuprofen, flurbiprofen, and indomethacin. *Pharm Res*. 2006;23:873–81.
51. Kalvass JC, Maurer TS, Pollack GM. Use of plasma and brain unbound fractions to assess the extent of brain distribution of 34 drugs: comparison of unbound concentration ratios to in vivo p-glycoprotein efflux ratios. *Drug Metab Dispos: the biological fate of chemicals*. 2007;35:660–6.
52. Gradishar WJ, Tjulandin S, Davidson N, Shaw H, Desai N, Bhar P, et al. Phase III trial of nanoparticle albumin-bound paclitaxel compared with polyethylated castor oil-based paclitaxel in women with breast cancer. *J Clin Oncol*. 2005;23:7794–803.
53. Marupudi NI, Han JE, Li KW, Renard VM, Tyler BM, Brem H. Paclitaxel: a review of adverse toxicities and novel delivery strategies. *Expert Opin Drug Saf*. 2007;6:609–21.